China Ocean Eng., Vol. 26, No. 4, pp. 669 – 684

DOI 10.1007/s13344-012-0050-0, ISSN 0890-5487

A Three-Dimensional Water Quality Model and Its Application to Jiaozhou Bay, China*

ZHANG Yan (张　燕)[a], SUN Ying-lan (孙英兰)[b, 1], YU Jing (余　静)[c],
YUAN Dao-wei (袁道伟)[d] and ZHANG Rui-jin (张瑞瑾)[a]

[a] *School of Ocean Science-Technology and Environment*, *Dalian Ocean University*, *Dalian 116023*, *China*
[b] *Ocean University of China*, *Qingdao 266003*, *China*
[c] *College of Physical and Environmental Oceanography*, *Ocean University of China*, *Qingdao 266003*, *China*
[d] *National Marine Environment Monitoring Center*, *Dalian 116023*, *China*

(Received 20 April 2010; received revised form 23 November 2011; accepted 2 February 2012)

ABSTRACT

A three-dimensional coupled physical and water quality model was developed and applied to the Jiaozhou Bay to study water quality involving nutrients, biochemical oxygen demand, dissolved oxygen, and phytoplankton that are closely related to eutrophication process. The physical model is a modified ECOM-si version with inclusion of flooding/draining processes over the intertidal zone. The water quality model is based on WASP5 which quantifies processes governing internal nutrients cycling, dissolved oxygen balance and phytoplankton growth. The model was used to simulate the spatial distribution and the temporal variation of water quality in the Jiaozhou Bay for the period of May 2005 to May 2006. In addition, the effect of reduction of riverine nutrients load was simulated and evaluated. The simulated results show that under the influence of nutrients discharged from river, the concentrations of nutrients and phytoplankton were higher in the northwest and northeast of the bay, and decreased from the inner bay to the outer. Affected by strong tidal mixing, the concentrations of all state variables were vertically homogeneous except in the deeper regions where a small gradient was found. Obvious seasonal variation of phytoplankton biomass was found, which exhibited two peaks in March and July, respectively. The variation of riverine waste loads had remarkable impact on nutrients concentration in coastal areas, but slightly altered the distribution in the center of the bay.

Key words: *water quality model*; *eutrophication*; *numerical simulation*; *three-dimensional*; *Jiaozhou Bay*

1. Introduction

Nutrients enrichment and eutrophication have attracted more and more concerns recently in many water bodies (Baird *et al*., 1995; Hermann *et al*., 1997; Arhonditsis *et al*., 2000). High concentrations of nitrogen and phosphorus can lead to periodic phytoplankton blooms and alteration of the natural trophic balance. The temporal variation and spatial distribution of nutrients in coastal areas are controlled by a complex physical-biological-chemical interaction process associated with external loading. Since these complicated processes are strongly nonlinearly coupled, studies of the nutrient-derived eutrophication usually rely on a water quality model with inclusion of inorganic and organic

* This work was supported by Qingdao Ocean and Fisheries Bureau.
1 Corresponding author. E-mail: zybetty@126.com

matter transformation and utilization. In addition, dissolved oxygen (DO) is another critical variable in evaluating the water quality in eutrophic water body. The low DO concentration directly affects survivals of fishes and thus destroys coastal waters healthy ecological balance. The distribution of DO is controlled by advection, turbulent mixing, reaeration, oxidation of organic matter, nitrification, phytoplankton photosynthesis and respiration, sediment oxygen demand (SOD), etc (Ambrose *et al*., 1993). Study of DO is often conducted by use of a water quality model. The water quality has been extensively examined in many estuaries and coastal areas (Zheng *et al*., 2004; Karim *et al*., 2002; Wang *et al*., 1999).

In recent decades, nutrient concentrations, nutrient ratios, and phytoplankton composition have notably changed in the Jiaozhou Bay due to the influence of human activities (Shen, 2001; Shen *et al*., 2006). Red tide has become a frequent event as the bay water is well-nourished. Some Jiaozhou Bay ecological models were a kind of box and one-dimensional model difficult for describing parameters with variability in space (Ren *et al*., 2003; Cui and Zhu, 2001). Three-dimensional physical-biological coupled models were developed with the advance in marine interdisciplinary research (Chen *et al*., 1999; Liu *et al*., 2007). These results allow understanding of the nutrient dynamics in the Jiaozhou Bay in many aspects and establish a foundation of further study. However, the processes in these model studies are still incomplete. For example, the intertidal zone is not included in the computation domain, and DO is not taken into account in previous coupled models. The objectives of this paper are to develop a three-dimensional coupled physical and water quality model of the Jiaozhou Bay and use it to identify and quantify how the physical, biological, and chemical processes controlling the spatial distribution and temporal variation of water quality components, and to test the sensitive effect of a reduction of the riverine waste loading. This model can help users understand and predict water quality responses to various pollution management decisions.

2. Description of Study Site

The Jiaozhou Bay (JZB), surrounded by the city of Qingdao, is the largest semi-enclosed water body along the South Yellow Sea coast of China (Fig. 1).

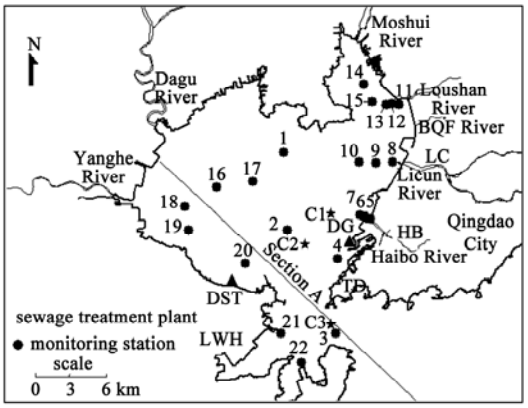

Fig. 1. Geometry and bathymetry of JZB. The filled circles are the water quality measurement stations in May, August, and October 2005. The heavy solid line is the section used for the model-data comparison. The filled triangles are tidal measurement stations. The filled stars are three current mooring sites. Filled flags denote locations of four waste treatment plants.

It is located in the southern part of the Shandong Peninsula. The bay has an area of about 423 km^2 (Liu, 1992) which is characterized by a large intertidal zone in the northwest and north regions. The major part of JZB is very shallow, smaller than 5 m, while the maximum depth, over 50 m, is located at the center of the bay mouth connecting to the Yellow Sea. The semidiurnal M_2 tide is the dominant tidal component which accounts for about 80% to 90% of current variation and kinetic energy within the bay. Strong tidal mixing results in nearly homogeneous vertical profiles of temperature and salinity (Ding, 1992). More than 10 small rivers enter JZB, among which the largest one is the Dagu River. Others passing through the urban area, such as the Lincun River, the Haibo River and the Loushan River, have become conduits for industrial and sanitary waste. The majority of effluent loadings to JZB are concentrated in the northern and eastern sections of the bay.

3. Coupled Physical and Water Quality Model

3.1 Physical Model

The physical model used in this study is a modified version of the three-dimensional estuarine and coastal ocean model developed originally by Blumberg (1986). The principal attributes of the model are as follows: (1) It contains an imbedded Mellor and Yamada (1982) level 2.5 turbulence closure sub-model to provide flow-dependent vertical mixing coefficients. (2) It uses a sigma coordinate in the vertical coordinate and a curvilinear orthogonal coordinate in the horizontal, allowing a better representation of irregular bottom topography and coastal geometry. (3) The model uses a semi-implicit method where the barotropic pressure gradient in the momentum equations and the horizontal velocity divergence in the continuity equation are treated implicitly. The implicit numerical algorithm permits time steps much larger than those based upon the CFL constraint. (4) It calculates terms of advection, Coriolis, baroclinic pressure gradient, and horizontal diffusion by use of explicit finite-difference scheme, and vertical diffusion term by using implicit finite-difference scheme, respectively. The latter eliminates time constraints for the vertical coordinate and permits the use of fine vertical resolution in the surface and bottom boundary layers. In addition, dry-wet grid technology is introduced to treat the tidal flood-ebb in tidal flat areas (Zheng *et al*., 2003; Wang *et al.*, 2009). The physical model outputs the hydrodynamic parameters (i.e., tidal elevation, current) to drive the transport process of state variables of water quality model.

3.2 Water Quality Model

The water quality model used in this study was built based on three-dimensional Water-quality Analysis Simulation Program (WASP5) developed originally by Ambrose *et al*. (1993). It simulates the transport and transformation reactions of up to eight state variables: ammonium nitrogen (NH_4), nitrate and nitrite nitrogen (NO_3), inorganic phosphorus (DIP), phytoplankton as carbon (PHYT), carbonaceous biochemical oxygen demand (CBOD), dissolved oxygen (DO), organic nitrogen (ON), and organic phosphorus (OP). They can be considered as the following interacting systems: phytoplankton kinetics, phosphorus cycle, nitrogen cycle, dissolved oxygen balance, and benthic-water column interactions. The conceptual framework for the water quality model is presented in Fig. 2.

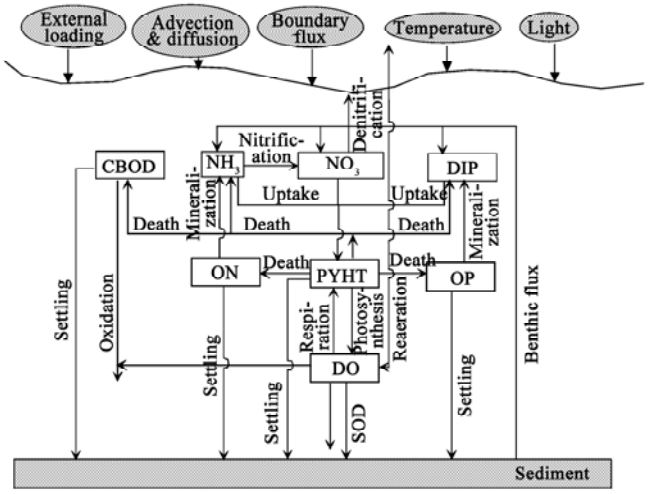

Fig. 2. Sketch map of water quality concept model.

The general mass balance equation is solved for each state variable. The governing equations of this model are given as:

$$\frac{\partial C_i}{\partial t}+u\frac{\partial C_i}{\partial x}+v\frac{\partial C_i}{\partial y}+(w-w_{is})\frac{\partial C_i}{\partial z}=\frac{\partial}{\partial x}\left(A_h\frac{\partial C_i}{\partial x}\right)+\frac{\partial}{\partial y}\left(A_h\frac{\partial C_i}{\partial y}\right)+\frac{\partial}{\partial z}\left(K_h\frac{\partial C_i}{\partial z}\right)+S_i+W_{0i}, \quad (1)$$

where C_i (i=1, 2, ⋯, 8) is corresponding to the concentrations of eight state variables; u, v, and w are the water velocity components corresponding to the conventional Cartesian coordinate system (x, y, z); w_{is} is the settling velocity of particulate organic matter; A_h and K_h are the coefficients of the horizontal viscosity and vertical eddy diffusion, respectively; W_{0i} is the external loading of the water quality components, and S_i is the function listed in Table 1 that represents the internal source or sink of the water quality components.

Some modifications to their original model have been made in our studies. First, we adopted the different temperature correction terms of phytoplankton growth rate, mineralization rate of dissolved organic nitrogen, and phytoplankton death rate. Second, instead of using modeling frameworks developed by WASP5, we adopted Steel's function to specify the effects of light attenuation. Finally, we used Ivlev formula (Chen, 2003) to describe the zooplankton grazing on phytoplankton in place of setting a constant grazing rate.

3.2.1 *Phytoplankton Kinetics*

Phytoplankton kinetics plays a central role in marine ecosystem. It is assumed that phytoplankton growth is limited by solar radiation, nutrients, and affected by ambient water temperature. The growth rate, G_P is specified via the following equation.

$$G_P=k_{gr}e^{\theta_{gT}}f(N)f(I), \quad (2)$$

where $f(N)$ is the nutrients limitation factor. All the individual nutrients are computed by a Michaelis-

Menten type expression, and the minimum value is chosen for the nutrient limiting factor, $f(N)=\min\left(\frac{C_1+C_2}{k_{\mathrm{mN}}+C_1+C_2},\frac{C_3}{k_{\mathrm{mP}}+C_3}\right)$. $f(I)$ is the light limitation factor, which is modeled by Steel's function, $f(I)=\frac{I}{I_s}\mathrm{e}^{1-I/I_s}$, where $I=I_0\mathrm{e}^{kz}$. The light extinction coefficient, k, is computed from the sum of the non-algal light attenuation (k_e), and the phytoplankton self-shading attenuation k_{eshd}. k_{eshd} can be expressed by the following equation.

$$k_{\mathrm{eshd}}=0.0088\,P_{\mathrm{Chl}}+0.054\,P_{\mathrm{Chl}}^{0.67}, \tag{3}$$

where P_{Chl} (μg/L) is phytoplankton chlorophyll concentration.

Table 1 Mathematical expression for the internal sources or sinks of the water quality variables

Mathematic expression for the internal sources or sinks
$S_1=a_{\mathrm{nc}}D_{\mathrm{p}}(1-f_{\mathrm{on}})C_4+k_{71}\mathrm{e}^{\theta_{71}T}\frac{C_4}{K_{\mathrm{mpc}}+C_4}C_7-G_{\mathrm{p}}a_{\mathrm{nc}}P_{\mathrm{NH_3}}C_4-k_{12}\theta_{12}^{(T-20)}\frac{C_6}{K_{\mathrm{NIT}}+C_6}C_1+B_1$;
$S_2=k_{12}\theta_{12}^{(T-20)}\frac{C_6}{K_{\mathrm{NIT}}+C_6}C_1-G_{\mathrm{p}}a_{\mathrm{nc}}(1-P_{\mathrm{NH_3}})C_4k_{2\mathrm{D}}\theta_{2\mathrm{D}}^{(T-20)}\frac{C_6}{K_{\mathrm{NO_3}}+C_6}C_2+B_2$;
$S_3=a_{\mathrm{pc}}D_{\mathrm{p}}(1-f_{\mathrm{op}})C_4+k_{83}\theta_{83}^{(T-20)}\frac{C_4}{K_{\mathrm{mpc}}+C_4}C_8-G_{\mathrm{p}}a_{\mathrm{pc}}C_4+B_3$;
$S_4=G_{\mathrm{p}}C_4-D_{\mathrm{p}}C_4-\frac{W_{4s}}{D}C_4$;
$S_5=a_{\mathrm{oc}}k_{1\mathrm{D}}\mathrm{e}^{\theta_{1\mathrm{D}}T}C_4-k_{\mathrm{D}}\theta_{\mathrm{D}}^{(T-20)}\frac{C_6}{K_{\mathrm{BOD}}+C_6}C_5-\frac{5}{4}\cdot\frac{32}{14}k_{2\mathrm{D}}\theta_{2\mathrm{D}}^{(T-20)}\frac{C_6}{K_{\mathrm{NO_3}}+C_6}C_2$;
$S_6=K_2(C_{\mathrm{s}}-C_6)-k_{\mathrm{D}}\theta_{\mathrm{D}}^{(T-20)}\frac{C_6}{K_{\mathrm{BOD}}+C_6}C_5-\frac{64}{14}k_{12}\theta_{12}^{(T-20)}\frac{C_6}{K_{\mathrm{NIT}}+C_6}C-\frac{SOD}{D}\theta_{\mathrm{s}}^{(T-20)}$ $+G_{\mathrm{p}}\left[\frac{32}{12}+\frac{48}{14}a_{\mathrm{nc}}(1-P_{\mathrm{NH_3}})\right]C_4-\frac{32}{12}k_{1\mathrm{r}}\theta_{1\mathrm{r}}^{(T-20)}C_4$;
$S_7=a_{\mathrm{nc}}D_{\mathrm{p}}f_{\mathrm{on}}C_4-k_{71}\mathrm{e}^{\theta_{71}T}\frac{C_4}{K_{\mathrm{mpc}}+C_4}C_7$;
$S_8=a_{\mathrm{pc}}D_{\mathrm{p}}f_{\mathrm{op}}C_4-k_{83}\theta_{83}^{(T-20)}\frac{C_4}{K_{\mathrm{mpc}}+C_4}C_8$.

The reduction rate of phytoplankton includes its endogenous respiration, death, and grazing by herbivorous zooplankton. It can be expressed as:

$$D_{\mathrm{P}}=k_{1\mathrm{r}}\theta_{1\mathrm{r}}^{(T-20)}+k_{1\mathrm{D}}\mathrm{e}^{\theta_{1\mathrm{D}}T}+R_{\mathrm{m}}(1-\mathrm{e}^{-\lambda C_4})Z(t), \tag{4}$$

where $Z(t)$ is the herbivorous zooplankton population grazing on phytoplankton, mgC/L. The annual variation of zooplankton population was specified based on observation data (Ren *et al*., 2003). The spatial distribution of zooplankton population was assumed uniform in the study area.

3.2.2 *Phosphorus Cycle*

Phosphate is taken up by phytoplankton for growth, and is incorporated into phytoplankton biomass. Phosphorus is returned from the phytoplankton biomass pool to dissolve and particulate organic phosphorus and dissolved inorganic phosphorus through endogenous respiration and

nonpredatory mortality. Organic phosphorus is converted to dissolve inorganic phosphorus at a temperature-dependent mineralization rate.

3.2.3 *Nitrogen Cycle*

Ammonia and nitrate are taken up by phytoplankton for growth, and incorporated into phytoplankton biomass. The rate at which each is taken up is a function of its concentration relative to the total inorganic nitrogen (NH_4 plus NO_3) available. Nitrogen is returned from the phytoplankton biomass pool to dissolve and particulate organic nitrogen and to ammonia through endogenous respiration and nonpredatory mortality. Organic nitrogen is converted to ammonia at a temperature-dependent mineralization rate, and ammonia is then converted to nitrate at a temperature- and oxygen-dependent nitrification rate. Nitrate may be converted to nitrogen gas in the absence of oxygen at a temperature- and oxygen-dependent denitrification rate. An ammonia preference factor for algal uptake of inorganic nitrogen is employed for physiological reasons. It can be expressed as:

$$P_{\mathrm{NH_3}} = C_1\left[\frac{C_2}{(K_{\mathrm{mN}}+C_1)\ (K_{\mathrm{mN}}+C_2)}\right] + C_1\left[\frac{K_{\mathrm{mN}}}{(C_1+C_2)\,(K_{\mathrm{mN}}+C_2)}\right]. \tag{5}$$

3.2.4 *Dissolved Oxygen Balance*

Dissolved oxygen is coupled to other state variables. The sources of oxygen considered are reaeration and evolution by phytoplankton during growth. The sinks of oxygen are algal respiration, oxidation of carbonaceous material from waste effluents, and nitrification. The following equation is used in the model to calculate DO saturation.

$$\begin{aligned}\ln C_{\mathrm{s}} = {} & -139.34 + (1.5757\times10^{5})\,T_{\mathrm{K}}^{-1} - (6.6423\times10^{7})\,T_{\mathrm{K}}^{-2} + (1.2438\times10^{10})\,T_{\mathrm{K}}^{-3} \\ & - (8.6219\times10^{11})\,T_{\mathrm{K}}^{-4} - 0.5535\times S\times(0.031929 - 19.428\,T_{\mathrm{K}}^{-1} + 3867.3\,T_{\mathrm{K}}^{-2}),\end{aligned} \tag{6}$$

where C_{s} is the saturation concentration of DO; S is the salinity, and T_{K} is the absolute temperature.

3.2.5 *Benthic-Water Column Interactions*

The decomposition of organic material in benthic sediment layer can have profound effects on the concentrations of oxygen and nutrients in the overlying waters. The decomposition of organic material releases nutrients to the sediment interstitial waters and also results in the exertion of an oxygen demand at the sediment-water interface. As a result, the fluxes from the sediment can be substantial nutrient sources or oxygen sinks to the overlying water column. B_1, B_2, B_3, and *SOD* represent bottom ammonium flux, bottom nitrate flux, bottom phosphate flux, and sediment oxygen demand, respectively. Spatially-variable observed fluxes are specified for ammonia, nitrate, phosphate, and *SOD* (Jiang *et al*., 2004; Zhang *et al*., 2004; Zhang *et al*., 2006).

3.3 Biological Parameters

Since biological parameters vary in a wide range with temporal and spatial dimensions, we first run the model with an initial setup of parameters, which were specified based on literature values (Ambrose *et al*., 1993; Zheng *et al*., 2004; Chen *et al*., 1999) and previous site-specific studies (Ren, 2003), and then were calibrated by using available observed data in 22 water quality measurement stations inside JZB in May 2005. Data series, the seasonal variability of the nutrients and

phytoplankton were collected to validate our model output (Figs. 6 and 7).The biological parameters used in water quality model are listed in Table 2.

Table 2 Parameters and constants for the water quality model

Notation	Description	Value	Unit
a_{nc}	Phytoplankton nitrogen to carbon ratio	0.18	Unitless
a_{pc}	Phosphorus to carbon ratio	0.024	Unitless
a_{oc}	Oxygen to carbon ratio in phytoplankton	32/12	Unitless
CCHL	Carbon-to-chlorophyll ratio	60	mgC/mgchla
C_s	DO saturation concentration	Eq.(6)	mgO/l
D_p	Phytoplankton death rate	Eq.(4)	d^{-1}
f_{on}	Fraction to the organic nitrogen pool	0.65	Unitless
f_{op}	Fraction to the organic phosphorus	0. 5	Unitless
f_{D5}	Fraction of dissolved CBOD	1.0	Unitless
f_{D7}	Fraction of dissolved ON	1.0	Unitless
f_{D8}	Fraction of dissolved OP	1.0	Unitless
G_p	Phytoplankton growth rate	Eq.(2)	d^{-1}
I_s	Optimal light intensity	90	W/m^2
k_{71}	Mineralization rate of dissolved organic nitrogen at 0℃	0.05	d^{-1}
k_{12}	Nitrification rate at 20℃	0.09	d^{-1}
k_{2D}	Denitrification rate at 20℃	0.09	d^{-1}
k_{83}	Mineralization rate of dissolved organic phosphorus at 20℃	0.22	d^{-1}
k_{gr}	Saturated growth rate of phytoplankton at 0℃	0.75	d^{-1}
k_{1r}	Average phytoplankton endogenous respiration rate constant at 20℃	0.125	d^{-1}
k_{1D}	Phytoplankton death rate at 0℃	0.018	d^{-1}
k_D	CBOD deoxygenation rate constant at 20℃	0.2	d^{-1}
k_{mN}	Nitrogen half-saturation constant for phytoplankton growth	0.01	mgN/L
k_{mP}	Phosphorus half-saturation constant for phytoplankton growth	0.006	mgP/L
K_{mpc}	Half-saturation constant for phytoplankton limitation	1.0	mgC/l
K_{NIT}	Half-saturation constant for oxygen limitation of nitrification	2.0	mgO_2/L
K_{NO_3}	Michaelis constant for denitrification	0.1	mgO_2/L
K_{BOD}	half-saturation concentration for oxygen limitation of CBOD oxidation	0.5	mgO_2/L
k_e	Non-algal light attenuation coefficient	0.8	m^{-1}
k_{eshd}	Algal light attenuation coefficient	Eq.(3)	m^{-1}
θ_{71}	Temperature coefficient for organic nitrogen mineralization rate at 0℃	0.04	Unitless
θ_{12}	Temperature coefficient for nitrification rate	1.08	Unitless
θ_{2D}	Temperature coefficient for denitrification rate	1.08	Unitless
θ_{83}	Temperature coefficient for organic phosphorus mineralization rate	1.08	Unitless
θ_{gr}	Temperature coefficient for phytoplankton growth rate	0.023	Unitless
θ_{1r}	Temperature coefficient for phytoplankton respiration rate	1.045	Unitless
θ_{1D}	Temperature coefficient for phytoplankton death rate	0.065	Unitless

Table 2 (continued)

Notation	Description	Value	Unit
θ_D	Temperature coefficient for deoxygenation death rate	1.047	Unitless
P_{NH_3}	Preference for ammonia uptake term	Eq.(5)	Unitless
W_{4s}	Settling velocity of phytoplankton	1.0	m/s
W_{5s}	Settling velocity of CBOD	0.5	m/s
W_{7s}	Settling velocity of particulate ON	0.5	m/s
W_{8s}	Settling velocity of particulate OP	0.5	m/s
R_m	Zooplankton maximum grazing rate	0.6	d^{-1}
λ	Ivlev constant for grazing	0.25	$(\mu mol/l)^{-1}$

3.4 Design of Numerical Experiments

The model domain covers the entire area of JZB with its open boundary located on the inner shelf of the Yellow Sea. The horizontal grids were designed by use of an orthogonal curvilinear transformation with total cells of 72×153. The horizontal resolution was about 240 m in the intertidal zone and about 800 m close to the open boundary. The 5 σ-levels were used in the vertical, which provided a vertical resolution of about 0.6 m near the coast and 10 m outside the bay. The time step used in the numerical computation was 186.3 s. The physical model was driven by the oscillation surface elevation with amplitudes and phases of the observed M_2 tide at the open boundary. The model included inputs of six tributaries and outfalls of four sewage treatment plants along the coast (Fig. 1). Based on measurements from Environment Monitoring Center of Qingdao and historic data (Zhao *et al*., 1997; Shen, 2002), we estimated the waste loads from rivers and waste treatment plants. Table 3 presents the yearly average external loads of major pollution sources in 2005.

Table 3 Yearly averaged riverine and waste treatment plants waste loads into JZB of NH_4, NO_3, DIP, COD, ON and OP

River	NH_4 flux (kg/d)	NO_3 flux (kg/d)	DIP flux (kg/d)	COD flux (kg/d)	ON flux (kg/d)	OP flux (kg/d)
Haibo	1513	370	120	17945	0	43.2
Licun	2716	468	200	25834	340	72.2
Banqiaofang (BQF)	1279	320	91	9500	0	32.7
Loushan	2067	600	47	33908	74	17.1
Moshui	2255	654	198	19483	118	71.4
Dagu	2685	1342	209	13805	58	75.3
Yanghe	1	1	1	210	7	0.3
Sewage treatment plant	NH_4 flux (kg/d)	NO_3 flux (kg/d)	DIP flux (kg/d)	COD flux (kg/d)	ON flux (kg/d)	OP flux (kg/d)
Tuandao (TD)	151	76	54	2744	913	19.3
Haibohe (HB)	4477	430	97	5159	0	35.0
Licunhe (LC)	129	954	83	4750	694	30.0
Lianwanhe (LWH)	191	28	13	946	0	4.6

Owing to the lack of CBOD measurement, chemical oxygen demand (COD) was simulated in the proportion 1:2 of concentration between CBOD and COD. The initial values of NH_4, NO_3, DIP, COD, ON, and OP were specified by use of the calculated results on the last day by running the model for three months with external loadings when the influence of river discharge reached a quasi-equilibrium state. Based on the observation, the initial values of DO and PHYT were assumed to be uniform in

numerical domain with values of 7.0 mgO_2/l and 0.06 mgC/l, respectively. Variables of water quality model are calculated after 3-D hydrodynamics fields are updated at each step. With input pollution loads, model-predicted tidal current field and the environmental forcing (light and temperature), the water quality model experiments started on May 1, 2005 and ran for one year.

4. Model Results

4.1 Tidal Simulation

The model-predicted tidal elevation and currents were compared directly with the observed data at two tidal stations and three current mooring sites in JZB, respectively (Table 4 and Fig. 3). Simulated and observed values were in a good agreement. The differences of computed and observed amplitudes and phases were 2.1 cm and 1.3º at Dagang, 2.9 cm and 1.7° at Dashitou. The application of the model to JZB grasps the tidal characteristics well. At the flood time the tidal current flowed northward with the strong water transport. At the ebb time the tidal current flowed southward out of JZB. Maximum horizontal velocities of around 100 cm/s occur at the bay mouth at the middle of the flooding and ebbing period. A detailed description of the results of the modeling tidal current can be found in Sun and Zhang (2001).

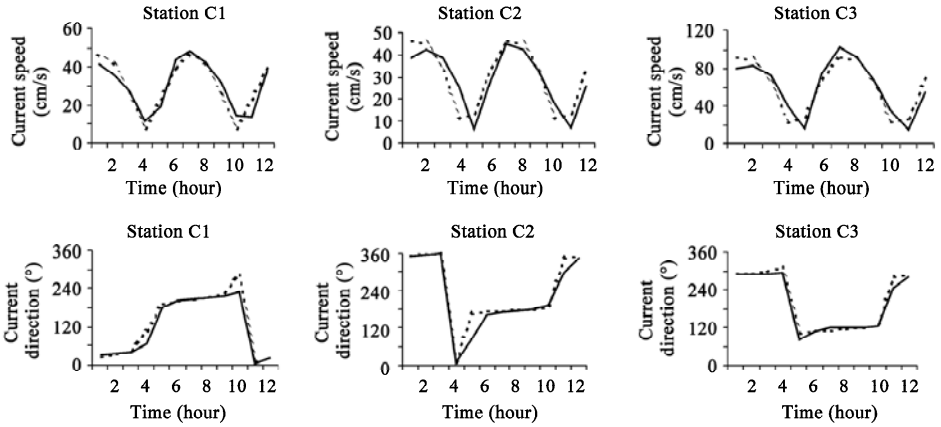

Fig. 3. Comparisons between the observed and model-predicted M_2 tidal currents at three mooring stations C1~C3. The model-predicted and observed values are presented by solid lines and dashed lines respectively.

Table 4 Comparison of measured and model-predicted M_2 tidal amplitudes and phases in JZB

Stations	Amplitude (cm)		Phase (°)	
	Measured	Model-predicted	Measured	Model-predicted
Dagang (DG)	126.4	128.5	132.8	131.5
Dashitou (DST)	125.3	128.2	131.9	133.6

4.2 Tidal-Cycle Average Distribution of Water Quality Constituents

In the standard run (the selected parameters are listed in Table 2), the horizontal distributions of all state variable near-surface concentrations as simulated on August 15, 2005 are presented (Figs. 4a and 4b). The model results show that the concentrations of NH_4 and NO_3 were higher in the coastal

area and decreased towards the center of the bay and the outer. Similarly, the concentration of DIP was higher in the north, northwest, and east of JZB than in the southern and central areas. The maximum values of NH_4, NO_3, and DIP were 1.58 mgN/l, 1.36 mgN/l and 0.127 mgP/l near river mouths, respectively, while dropped to 0.037 mgN/l, 0.142 mgN/l, and 0.006 mgP/l at the mouth of the bay. Higher phytoplankton concentration appeared mainly in the northwest and northeast near-shore area, with extreme value exceeding 1.0 mgC/l near the mouth of Moshui River, and the lower was found in the south of JZB. Phytoplankton concentration was higher inside the bay than that of the outer. The synoptic distribution of the model-predicted near-surface DO concentration showed the reverse patterns as that of other water quality components. The DO concentration was high-spatially variable, which was lower with a value of smaller than 5 mgO_2/l near the mouth of Moshui River and Dagu River. It increased southward across the bay with the highest value of larger than 7.0 mgO_2/l.

The simulated vertical distributions of the water quality components on Section A on August 15, 2005 are presented in Fig. 5. The modeling results show that the distributions of NH_4, DIP, COD, and DO were well-mixed vertically. The distribution of NO_3 was uniform vertically except in deep regions where a slight increase from surface to bottom was found. Inversely the concentration of phytoplankton near the surface was a little higher than that near the bottom at the mouth of JZB. The concentrations of NH_4, NO_3, DIP, phytoplankton, and COD decreased with distance from the coast. However, DO concentration varied the other way round.

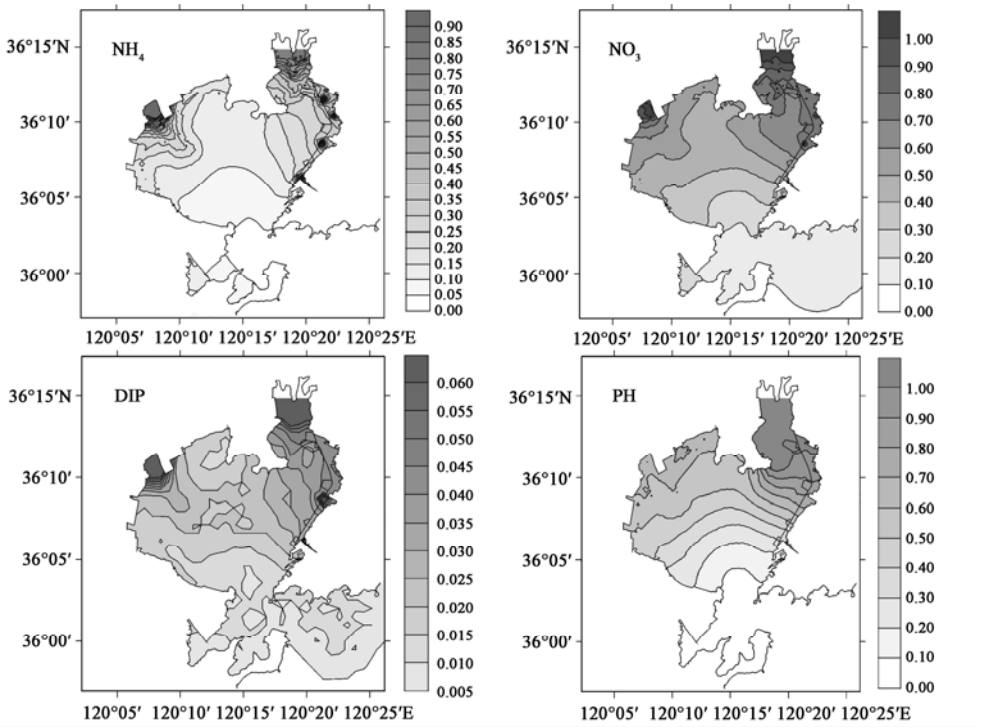

Fig. 4a. Tidal averaged surface distribution of NH_4, NO_3, DIP, and PHYT, in JZB on August 15, 2005.

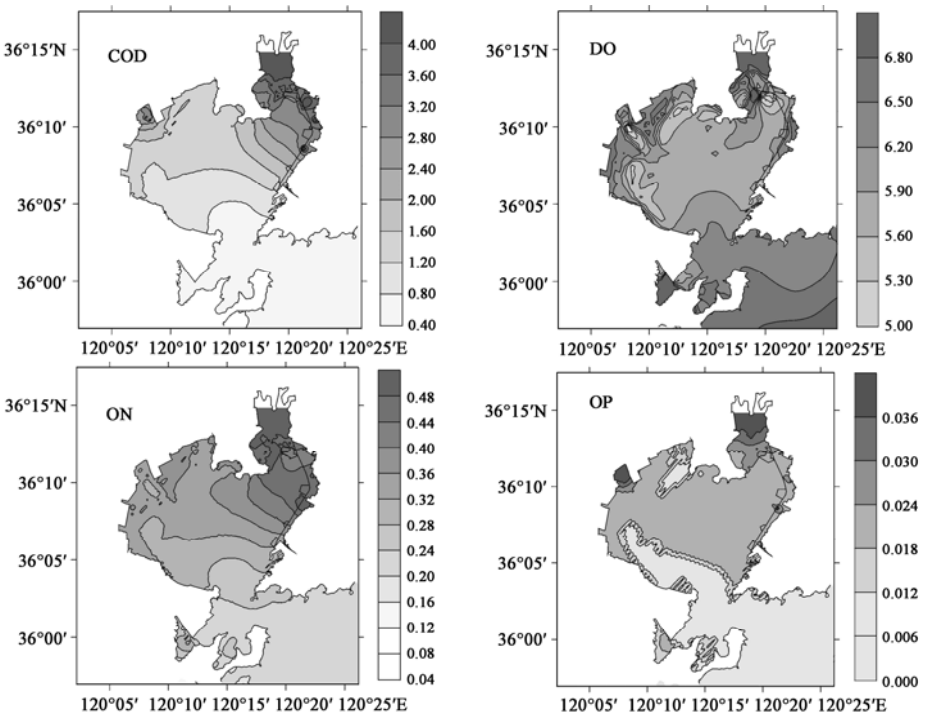

Fig. 4b. Tidal averaged surface distribution of CBOD, DO, ON, and OP in JZB on August 15, 2005.

Our model results of NH_4 and DIP accord basically with the observed seasonal variation at both stations. The concentration of NH_4 showed a decreasing trend from May to July in 2005. Subsequently with the growth of phytoplankton NH_4 was depleted, reaching the lower level in August. NH_4 increased in autumn, and accumulated in winter. In spring, the NH_4 concentration began to reduce along with the increasing phytoplankton content. The DIP temporal variation showed the similar pattern as NH_4. The relatively poor simulation of NO_3 concentration might be related to the lack of knowledge about nitrification in the water column. The simulation of phytoplankton for both stations was in a good agreement with the range given by the measurements (Li *et al*., 2005). An obvious seasonal variation of phytoplankton concentration was found, which exhibited two peaks during the study period. From May 2005, the phytoplankton concentration increased with the increasing water temperature, and reached the annual highest concentration in July with the extreme value of 0.57 and 0.21 mgC/l at Station 1 and Station 2, respectively. Then it decreased gradually, reaching the lower level in winter with values of only 0.2 and 0.09 mgC/l at Station 1and Station 2, respectively. With the increasing nutrients concentration, the second peak occurred in March 2006 with the higher value of 0.38 and 0.17 mgC/l at Station 1 and Station 2. Phytoplankton growth is limited by nutrients, solar radiation, and affected by ambient water temperature. The simulated maximum phytoplankton postpones the observation data by about one month in spring. The general decline of the nutrients with increasing phytoplankton indicates that the phytoplankton growth has an important impact on the change of nutrients. Thus the appearance of NH_4 concentration valley was delayed about two months compared with the observation in spring.

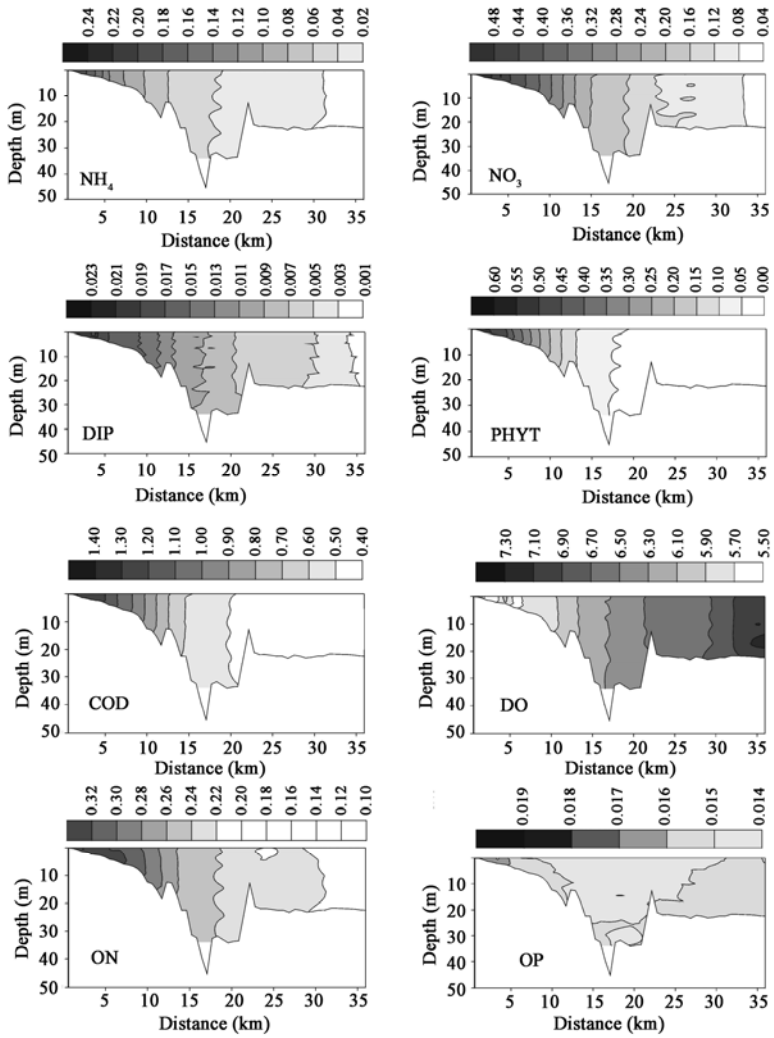

Fig. 5. Tidal averaged vertical distribution of NH_4, NO_3, DIP, PHYT, CBOD, DO, ON, and OP on Section A on August 15, 2005. The distance increases toward the outer bay.

The distributions and variation of model-predicted ON and OP are not further discussed. One of the reasons is that there are very few observational data of ON and OP available for JZB, nor do we have any data for model and data comparison. The simulations of other state variable are in good agreement with measurements.

4.3 Effects of External Loading

Scenarios have been analyzed to examine the effect of reduction of the riverine and sewage treatment plant nutrients load. All scenario model runs were conducted in the same way as the standard one. The simulated results represent the water quality model in a new quasi-equilibrium state, which corresponds to the new forcing. Three different scenario runs were conducted: applying 25%, 50% and 75% reduction of waste loads in scenario A, B, and C, respectively.

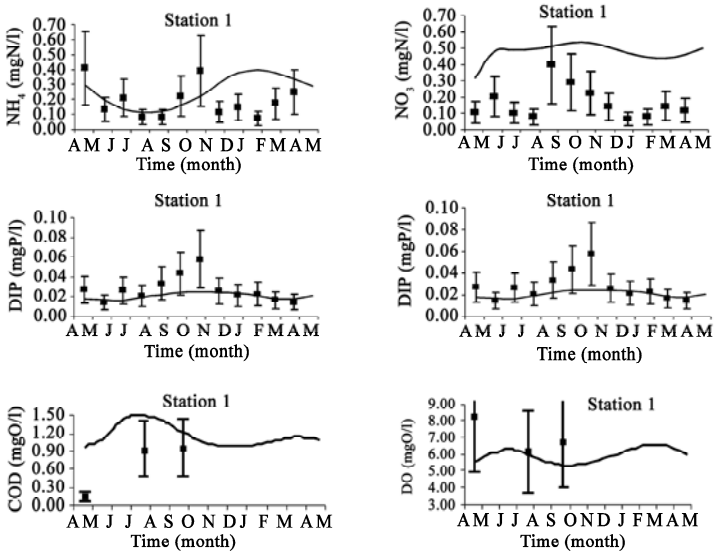

Fig. 6. Simulated concentrations of NH_4, NO_3, DIP, PHYT, COD, and DO at Station 1 from May 2005 to May 2006 were compared with monthly mean values derived from measurements. The measurements from Li *et al*. (2005) and Environment Monitoring Center of Qingdao (2005) are presented in the form of average value and ranges defined by 50% error. The filled squares indicate the observed values. The model-predicted values are presented by solid lines.

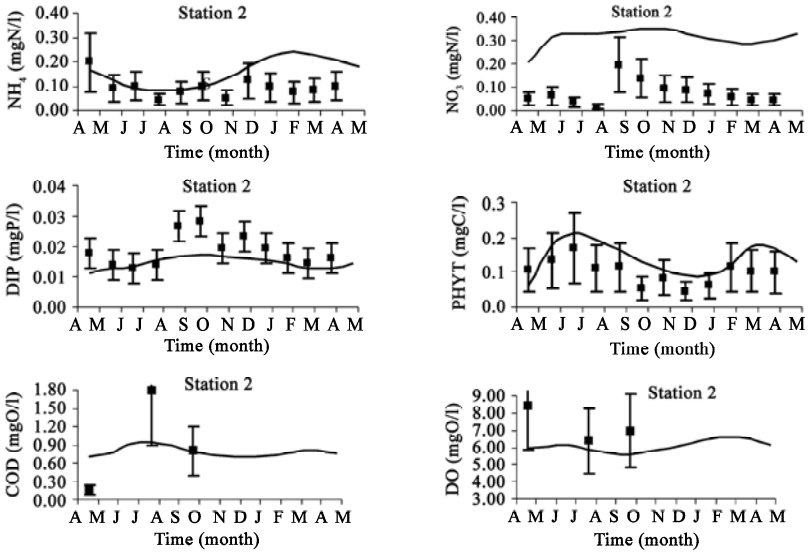

Fig. 7. Simulated concentrations of NH_4, NO_3, DIP, PHYT, COD, and DO at Station 2 from May 2005 to May 2006 were compared with monthly mean values derived from measurements. The measurements from Li *et al*. (2005) and Environment Monitoring Center of Qingdao (2005) are presented in the form of average value and ranges defined by 50% error. The filled squares indicate the observed values. The model-predicted values are presented by solid lines.

The results showed that the influence of riverine flux variation was distinct in the east, while it was relatively faint in the south of the Bay. Phytoplankton was most sensitive to the change of land-source pollutant input, while dissolved oxygen was relatively beef-witted. In Table 5, the concentrations of NH_4, NO_3, DIP, phytoplankton, DO, ON, and OP at Stations 1, 2, 3, 7, and 16 are

shown for the three different scenarios in 2005. These stations show a reduction of NH_4 concentration of more than 6.3% in scenario A, about 12.5% to 29.3% in scenario B, and from 18.6% to 43.1% in scenario C in comparison with the standard run. The variation of riverine waste load had a large effect on phytoplankton content, which ranged from 40.1% to 79.8% in scenario C. It was almost no effect on DO concentration, which ranged from –0.4% to 3.5% in scenario C. As expected, the higher effect of the reduced external loads was found at Stations 7 and 16 near the estuary. It was of relatively insignificant influence at southern Station 3. In general, the difference was small at the offshore stations, which can be seen for other water quality components listed in Table 5.

Table 5 Comparisons of NH_4, NO_3, DIP, phytoplankton, DO, ON, and OP concentration from three different scenarios in 2005 (the numbers in brackets denote the reduction in percentage compared with the standard run which is abbreviated to std. run in Table 5)

Station No.	Scenarios	NH_4	NO_3	DIP	PHYT	COD	DO	ON	OP
1	Std. run	0.256	0.4746	0.021	0.349	1.16	5.91	0.267	0.019
	Scenario A	0.231(9.7)	0.4226(11.0)	0.016(20.0)	0.268(23.3)	0.94(19.5)	5.87(0.7)	0.244(8.5)	0.017(7.4)
	Scenario B	0.209(18.5)	0.3738(21.2)	0.013(38.1)	0.173(50.3)	0.69(40.7)	5.80(1.9)	0.217(18.5)	0.016(15.7)
	Scenario C	0.187(27)	0.3281(30.9)	0.009(55.5)	0.076(78.1)	0.43(62.7)	5.72(3.3)	0.187(29.9)	0.014(24.2)
2	Std. run	0.157	0.3121	0.015	0.141	0.78	6.08	0.240	0.017
	Scenario A	0.141(10.0)	0.2819(9.7)	0.012(18.6)	0.110(21.9)	0.66(15.4)	6.09(−0.1)	0.227(5.4)	0.016(4.4)
	Scenario B	0.126(19.4)	0.2535(18.8)	0.009(35.9)	0.074(47.4)	0.53(32.2)	6.09(−0.2)	0.212(11.8)	0.015(9.2)
	Scenario C	0.112(28.6)	0.2268(27.3)	0.007(52.9)	0.037(73.6)	0.39(49.7)	6.08(−0.1)	0.195(19.0)	0.015(14.2)
3	Std. run	0.055	0.1351	0.006	0.038	0.49	6.63	0.214	0.015
	Scenario A	0.052(6.3)	0.1275(5.6)	0.005(12.0)	0.034(12.2)	0.46(5.4)	6.64(−0.1)	0.210(1.6)	0.015(1.0)
	Scenario B	0.048(12.5)	0.1203(10.9)	0.005(23.0)	0.028(26.1)	0.43(11.3)	6.65(−0.3)	0.206(3.5)	0.015(1.5)
	Scenario C	0.045(18.6)	0.1136(15.9)	0.004(34.6)	0.023(40.1)	0.40(17.5)	6.66(−0.4)	0.202(5.6)	0.015(3.5)
7	Std. run	0.281	0.4269	0.024	0.238	1.21	5.94	0.268	0.020
	Scenario A	0.239(15.0)	0.3759(12.0)	0.019(21.4)	0.188(21.2)	0.98(18.9)	5.95(−0.3)	0.248(7.5)	0.018(7.4)
	Scenario B	0.199(29.3)	0.3276(23.3)	0.014(41.2)	0.126(47.2)	0.74(39.3)	5.95(−0.2)	0.224(16.3)	0.017(15.3)
	Scenario C	0.160(43.1)	0.2822(33.9)	0.009(60.2)	0.058(75.7)	0.48(60.5)	5.92 (0.3)	0.197(26.4)	0.015(23.7)
16	Std. run	0.343	0.5080	0.025	0.350	1.13	6.20	0.253	0.020
	Scenario A	0.305(10.9)	0.4500(11.4)	0.020(19.9)	0.261(25.5)	0.90(19.8)	6.14(1.0)	0.233(8.1)	0.018(9.0)
	Scenario B	0.269(21.5)	0.3948(22.3)	0.015(38.8)	0.164(53.3)	0.67(41.0)	6.06(2.3)	0.209(17.6)	0.017(18.6)
	Scenario C	0.229(33.3)	0.3419(32.7)	0.010(57.9)	0.071(79.8)	0.42(62.5)	5.98(3.5)	0.182(28.0)	0.015(28.5)

5. Discussion

A coupled physical and water quality model was developed to study how the physical, biological, and chemical processes to control the distribution and variation of water quality components in JZB in 2005. The physical model is driven by M_2 tidal elevation at the open boundary, and the water quality model is based on WASP5 including the processes of phytoplankton kinetics, nutrients (phosphorus and nitrogen) cycle, DO balance, sediment oxygen demand, and nutrients fluxes from the bottom sediment. With the input of pollution loading and the environmental forcing (lighting and temperature), the water quality model experiments started on May 1, 2005 and ran for one year.

The model results show that the synoptic distribution of water quality components was significantly affected by physical, biological, and chemical processes. Strong tidal mixing caused ammonia, COD, DO, ON, and OP to be well-mixed in the vertical. The bottom concentrations of NO_3 and DIP were a little higher than that of the surface in deeper regions for inclusion of nutrient fluxes at water-sediment interface. The light intensity to which the phytoplankton is exposed is not uniform at the optimum

value. On the surface and near-surface of the air-water interface, photoinhibition will occur at high light intensities, whereas at depths below the euphotic zone light is not available for photosynthesis due to natural and algal-related turbidity. Thereby a slight decrease of phytoplankton content from surface to bottom was found in the deeper regions. Under the influence of river discharges and tidal motion, the concentrations of nutrient and phytoplankton were higher in the northwest, northeast, and north of the bay near river mouths and decreased from the inner bay to the outer. However, DO concentration showed the reverse patterns probably due to weaker nitrification and oxidation processes in the outer bay.

Comparison of simulated results with measurements shows a good agreement for NH_4, DIP, and phytoplankton which exhibit a clear annual cycle. Phytoplankton biomass was higher in summer and lower in winter. The seasonal variability of water temperature and light intensity has a direct effect on the phytoplankton growth. With nutrient accumulation in winter phytoplankton biomass increased in spring reaching the peak in March 2006. As phytoplankton growing, for physiological reasons the preferred form is ammonia nitrogen. Model results reveal that there was negative correlation between ammonia concentration and phytoplankton biomass.

In the scenario runs, with different reductions of the river nutrients loading, the higher effects were observed at the near-shore stations. The influence was less at the stations in the center and south of the bay. The river and waste treatment plant discharge variation has greater impact on phytoplankton biomass which reduced 79.8% at Station 16 in scenario C. Secondly nutrients concentration was influenced remarkably. However, there is little influence on DO concentration. As a result, to reduce waste loads from land is an effective way against phytoplankton bloom.

Acknowledgments - The research was conducted as a component of the program on Marine Environment Protection Planning of Qingdao. We wish to acknowledge the strong support of ZHENG Lian-yuan, who allowed us to use his modified WASP5 code, and provided technical guide and suggestions during model development. We also wish to thank ZHANG Xue-qing and ZOU Li for their comments and suggestions on water quality simulation.

References

Ambrose, R. B., Wool, T. A. and Martin, J. L., 1993. *The Water Quality Analysis Simulation Program*, *WASP5*, *Part A*: *Model Documentation*, *U.S.*, Environmental Protection Agency, Athens, Georgia.

Arhonditsis, G., Tsirtsis, G., Angelidis, M. O. and Karydis, M., 2000. Quantification of the effects of nonpoint nutrient sources to coastal marine eutrophication: applications to a semi-enclosed gulf in the Mediterranean Sea, *Ecological Modelling*, **129**(2-3): 209~227.

Baird, D., Ulanowicz, R. E. and Boynton, W. R., 1995. Seasonal nitrogen dynamics in the Chesapeake Bay: a network approach, *Estuar. Coast. Shelf Sci.*, **41**(2): 137~162.

Blumberg, A. F., 1986. *A Primer of ECOM-si,* Technical Report, HydroQual, Inc Mahwah, New Jersey.

Chen, C. S., Ji, R. B., Zheng, L. Y., Zhu, M. Y. and Rawson, M., 1999. Influence of physical process on the ecosystem in Jiaozhou Bay: A coupled physical and biological model experiment, *J. Geophys. Res.*, **104**(C12): 29925~29949.

Chen, C. S., 2003. *Marine Ecosystem Dynamics and Modeling*, Higher Education Press, Beijing. (in Chinese)

Cui, M. C. and Zhu, H., 2001. Coupled physical-ecological modeling in the central part of Jiaozhou Bay II. Coupled with an ecological model, *Chinese Journal of Oceanology and Limnology*, **19**(1): 21~28.

Ding, W. L., 1992. Tides and tidal currents, in: Liu, R Y, eds., *Ecology and Biological Resources of Jiaozhou Bay*, Science Press, Beijing, 39~57. (in Chinese)

Jiang, F. H., Wang, X. L., Shi, X. Y., Zhu, C. J., Hu, H. Y. and Han, X. R., 2004. Benthic exchange rates and fluxes of dissolved inorganic nitrogen at the sediment-water interface in Jiaozhou Bay, *Marine Sciences*, **28**(4): 13~18. (in Chinese)

Karim, M. R., Sekine, M. and Ukita, M., 2002. Simulation of eutrophication and associated occurrence of hypoxic and anoxic condition in a coastal bay in Japan, *Mar. Pollut. Bull.*, **45**(1-12): 280~285.

Lenhart, H. J., Radachm, G. and Ruardij, P., 1997. The effects of river input on the ecosystem dynamics in the continental coastal zone of the North Sea using ERSEM, *J. Sea Res.*, **38**(3-4): 249~274.

Li, C. L., Zhang, F., Shen, X., Yang, B., Shen, Z. L. and Song, S., 2005. Concentration, distribution and annual fluctuation of chlorophyll-a in the Jiaozhou Bay, *Oceanologia et Limnologia Sinica*, **36**(6): 499~506. (in Chinese)

Liu, R. Y., 1992. Characteristics of physical environmental of Jiaozhou Bay, in: Liu, R. Y., eds. *Ecology and Biological Resources of Jiaozhou Bay*, Science Press, Beijing, 2~3. (in Chinese)

Liu, Z., Wei, H., Bai, J., Zhang, J., Liu, D. Y. and Liu, S. M., 2007. Nutrients seasonal variation and budget in Jiaozhou Bay, China: A 3-dimensional physical – Biological coupled model study, *Water Air Soil Pollut: Focus*, **7**(6): 607~623.

Mellor, G. L. and Yamada, T., 1982. Development of a turbulence closure models for geophysical fluid problems, *Rev. Geophys. Space Phys.*, **20**(4): 851~875.

Ren, L., Zhang, M. P., Brockmann, H. U. and Feng, S. Z., 2003. Pelagic nitrogen cycling in Jiaozhou Bay, a model study I: The conceptual model, *Chinese Journal of Oceanology and Limnology*, **21**(4): 358~367.

Shen, Z. L., 2001. Historical changes in nutrient structure and its influences on phytoplantkon composition in Jiaozhou Bay, *Estuar. Coast. Shelf Sci.*, **52**(2): 211~224.

Shen, Z. L., 2002. Long-term changes in nutrient structure and its influences on ecology and environment in Jiaozhou Bay, *Oceanologia et Limnologia Sinica*, **33**(3): 322~331. (in Chinese)

Shen, Z. L., Liu, Q., Wu, Y. L. and Yao, Y., 2006. Nutrient structure of seawater and ecological responses in Jiaozhou Bay, China, *Estuar. Coast. Shelf Sci.*, **69**(1-2): 299~307.

Sun, Y. L. and Zhang, Y. M., 2001. A three dimensional variable boundary numerical tidal model for Jiaozhou Bay, *Oceanologia et Limnologia Sinica*, **32**(4): 355~362. (in Chinese)

Wang, P. F., Martin, J. and Morrison, G., 1999. Water quality and eutrophication in Tampa Bay, Florida, *Estuar. Coast. Shelf Sci.*, **49**(1): 1~20.

Wang, C., Zhang, X. Q. and Sun, Y. L., 2009. Numerical simulation of water exchange characteristics of the Jiaozhou bay based on a three-dimensional Lagrangian model, *China Ocean Eng.*, **23**(2): 277~290.

Zhang, X. L., Zhu, M. Y., Tang, T. Y., Wang, Y., Liu, G. and Martin, J.-L. M., 2004. Fluxes of nutrients at sediment-water in Sanggou Bay and Jiaozhou Bay in summer, *Marine Environmental Science*, **23**(1): 1~4. (in Chinese)

Zhang, X. L., Zhu, M. Y., Chen, S., Grant, J. and Martin, J. -L., 2006. Study on sediment oxygen consumption rate in the Sanggou Bay and Jiaozhou Bay, *Advances in Marine Science*, **24**(1): 91~96. (in Chinese)

Zhao, X. D., Zhu, C. J., Ju, P. and Shi, Z. L., 1997. The forms and concentrations of phosphorus in seawater in the eastern Jiaozhou Bay, *Marine Science*, (6): 53~56. (in Chinese)

Zheng, L. Y., Chen, C. S. and Liu, H. D., 2003. A modeling study of the Satilla River estuary, Georgia. I: Flooding-drying process and water exchange over the salt marsh-estuary-shelf complex, *Estuar. Coast.*, **26**(3): 651~669.

Zheng, L. Y., Chen, C. S. and Zhang, F. Y., 2004. Development of water quality model in the Satilla River estuary, Gerogia, *Ecol. Model.*, **178**(3-4): 457~482.